RSC Advances

COMMUNICATION

View Article Online
View Journal | View Issue

Cite this: *RSC Adv.*, 2015, **5**, 22300

Synthesis of highly dispersed cobalt catalyst for hydroformylation of 1-hexene†

Bin Wang, Jian-Feng Chen and Yi Zhang*

Received 25th December 2014
Accepted 11th February 2015

DOI: 10.1039/c4ra17035k

www.rsc.org/advances

Highly dispersed Co/SiO_2 catalysts were prepared using an ethylene glycol (EG) modified silica support. The modified SiO_2 support significantly promoted the dispersion of supported cobalt and adding a small amount of Ru increased the reducibility of the highly dispersed cobalt oxide. The $Co–Ru/SiO_2$ (EG) catalyst exhibited 3 times higher 1-hexene conversion and 18 times higher heptanal yield than the conventional Co/SiO_2 catalyst.

Hydroformylation is one of the most important syngas-related reactions, and the formed aldehydes are valuable final products and intermediates in the synthesis of bulk chemicals, such as alcohols, esters and amines.[1] This reaction could be catalyzed by transition metal complexes, such as Co and Ru, and involves the addition of hydrogen and carbon monoxide to olefins, yielding aldehydes.[2] Cobalt complexes are extensively applied in this reaction due to its high activity and low cost. All current commercial processes are based on homogeneous catalysts, mostly using rhodium. The successful development of a heterogeneous catalyst for hydroformylation could avoid the drawbacks of homogeneous catalyst, such as very high pressure, the catalyst separation and recovery steps.

Supported cobalt catalysts were known to be highly active for Fischer–Tropsch synthesis.[3,4] However, the supported cobalt catalysts always exhibit low catalytic activity and selectivity in olefin hydroformylation.[5,6] The hydroformylation activity of cobalt catalyst depended on the particle size and the number of active sites.[7–9] Therefore, cobalt must be in a highly dispersed form in order to improve the CO insertion reaction and increase amount of active sites. Synthesis of highly dispersed cobalt requires strong interaction between the support and the cobalt precursors, but these strong interactions result in cobalt species that are difficult to be reduced.[10] Many efforts have been devoted to improve the dispersion and the reducibility of supported cobalt particles.[11] As our previous report, the concentration, distribution, and nature of hydroxyl groups (silanols) on the silica surface played important roles in the dispersion of supported metal on the silica.[12,13] Pretreatment of silica by EG was found to increase the isolated Si–OH ratio on the silica surface, leading to the formation of smaller particles.[14,15] On the other hand, noble metal promoters could be reduced at a lower temperature than cobalt oxides, and shifted the reduction peaks of cobalt species to lower temperatures. Thus, adding small amounts of noble metals have been found to significantly promote the reduction degree of cobalt oxides, presumably by hydrogen spillover from Ru surface to cobalt oxides.[16,17]

In this study, the highly dispersed Co/SiO_2 catalysts were prepared using a silica support modified by ethylene glycol (EG). In order to improve the reducibility of highly dispersed cobalt, a small amount of Ru was added to the Co/SiO_2 catalysts. The obtained supported cobalt catalysts were tested in slurry phase hydroformylation of 1-hexene and the promotional effects of EG pretreatment and added Ru on catalytic performances were investigated by XRD, TEM, H_2-TPR, oxygen titration, H_2 chemsorption, XPS and *in situ* CO-DRIFT.

Typically, various Co/SiO_2 catalysts were prepared by the incipient wetness impregnation of aqueous of cobalt nitrate onto SiO_2 support (pore volume: 1.061 mL g^{-1}, pore diameter: 6.7 nm, specific surface area: 451 m^2 g^{-1}). The silica supports were pretreated with EG at room temperature for 1 h by incipient wetness impregnation method. And then, the samples were dried in air at 393 K for 12 h. A 10 wt% Co/SiO_2 catalyst was prepared as the following steps: a certain amount of $Co(NO_3)_3 \cdot 6H_2O$ was dissolved in water and then the cobalt nitrate aqueous solution was impregnated on the support. The obtained samples were dried in air at 393 K for 12 h and calcined at 673 K for 2 h with a heating rate of 2 K min^{-1}. The noble metal Ru promoted Co/SiO_2 catalysts were prepared by co-impregnation of cobalt nitrate and ruthenium chloride aqueous solution on SiO_2 support while other preparing procedures were

State Key Laboratory of Organic–Inorganic Composites, Research Centre of the Ministry of Education for High Gravity Engineering and Technology, Beijing University of Chemical Technology, Beijing 100029, China. E-mail: yizhang@mail.buct.edu.cn; Fax: +86 10 64423474; Tel: +86 10 64447274

† Electronic supplementary information (ESI) available. See DOI: 10.1039/c4ra17035k

constant. The loading of Ru promoter was 1 wt%. Before hydroformylation reaction, the catalysts were reduced by hydrogen at 673 K for 10 h and passivated by 1% oxygen diluted with nitrogen at room temperature. The prepared catalysts were denoted as Co/SiO_2, Co/SiO_2 (EG), $Co–Ru/SiO_2$ and $Co–Ru/SiO_2$ (EG), where EG indicated that the silicate supports were pretreated by EG.

XRD patterns of different catalysts are shown in Fig. 1. As shown in Fig. 1, the catalysts prepared from EG modified silica support exhibited very weak and broad peaks of cobalt than that of conventional catalyst. It indicated that the interaction between supported cobalt and silica support was stronger on EG modified silica than on conventional silica, resulting in highly dispersed cobalt oxide which was difficult to be reduced to metal cobalt. For the Ru added catalysts, the $Co–Ru/SiO_2$ (EG) catalyst still exhibited very weak and broad peaks of cobalt, indicating the cobalt particle size of this catalyst was still small due to EG modification of silica support. It should be mentioned that the reduced catalysts used here were in the passivated form where the reduced metallic cobalt particles were covered by a tailor-made oxidation layer before being ground in agate mortar for XRD measurement. Some cobalt oxides from the oxidation layer might exist besides the originally unreduced cobalt oxide.

TEM images of passivated catalysts were shown in Fig. 2. The average particle size of the supported Co was also determined by TEM. The average metallic Co particle size of Co/SiO_2 (EG) and $Co–Ru/SiO_2$ (EG) catalyst were 3.4 nm and 3.8 nm, respectively, as compared in Table 1. The dispersion of supported Co was calculated by the average particle size of Co, as shown in Table 1. It was found that the catalysts pretreated by EG had smaller particle sizes and realized almost 3 times higher dispersion than conventional one, indicating that EG pretreatment could improve the dispersion of supported Co. As previously reported,[12–15] EG pretreatment of SiO_2 decreased the coverage of Si–OH on the surface of support and increased the interaction between supported cobalt particles and silica, resulting in higher supported cobalt dispersion. The metallic cobalt

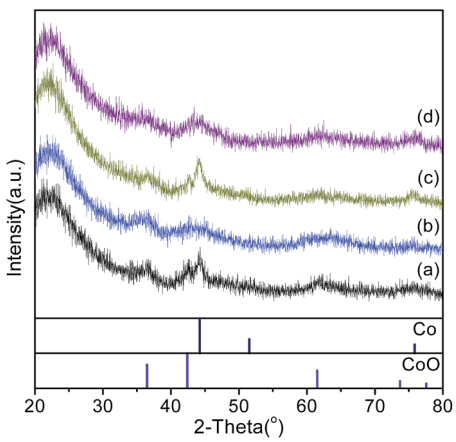

Fig. 1 XRD patterns of supported cobalt catalysts: (a) Co/SiO_2, (b) Co/SiO_2 (EG), (c) $Co–Ru/SiO_2$, and (d) $Co–Ru/SiO_2$ (EG).

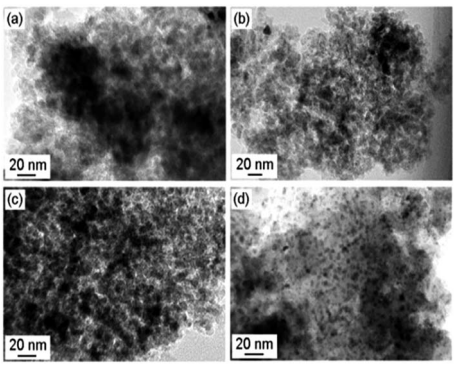

Fig. 2 TEM images of the prepared catalysts: (a) Co/SiO_2, (b) Co/SiO_2 (EG), (c) $Co–Ru/SiO_2$, and (d) $Co–Ru/SiO_2$ (EG).

particles of $Co–Ru/SiO_2$ catalyst were slightly larger than that of Co/SiO_2, which should be attributed to the fact that added Ru induced cobalt particles sintering during the reduction.[18] Therefore, addition of Ru would slightly decrease the dispersion of supported Co. However, for catalyst $Co–Ru/SiO_2$ (EG), the average cobalt particle size was still small and almost the same to that of Co/SiO_2 (EG) catalyst. It is considered that smaller cobalt particle size was advantageous to the adsorption of linear-bonded CO and the insertion of CO during the hydroformylation reaction.

The reduction performances for various catalysts were determined by temperature programmed reduction (TPR), as shown in Fig. 3. Co/SiO_2 catalyst undergoes two typical steps during reduction, which were identified as conversion of Co_3O_4 to CoO followed by conversion of CoO to Co. The peak locating at higher than 900 K should be the reduction of cobalt silicates, which strongly interacted with support.[19] The first reduction peak of Co/SiO_2 (EG) located at slightly lower temperature than that of Co/SiO_2. However, the second reduction peak was very broad and located at 650 K to 850 K, and the third reduction peak (above 900 K) became very strong and broad. These results indicated that the modification of silica support significantly enhanced the interaction between supported cobalt and silica, leading to formation of very small and difficult to be reduced cobalt particles. For catalyst $Co–Ru/SiO_2$, the reduction peak at about 434 K should be the reduction of ruthenium species, and the two reduction peaks for cobalt oxides shifted to lower temperatures and formed a broad peak in the range of 450–570 K indicating that addition of small amount of Ru significantly improved the reducibility of the obtained catalyst, which could be explained by hydrogen spillover from Ru to cobalt oxides.[20,21] Similar changes caused by Ru addition could also be observed on the catalyst of $Co–Ru/SiO_2$ (EG) which exhibited only one broad reduction peak located from 400 K to 600 K with several shoulder peaks, indicating the reduction of various cobalt species was significantly improved by added Ru.

The reduction degrees of the catalysts were calculated according to the oxygen titration at 673 K and H_2-TPR from 323 K to 673 K, as shown in Table 1. It is shown that the reduction degrees obtained through oxygen titration and TPR were similar to each other. EG pretreatment of support made

Table 1 Properties of various catalysts

Catalyst	Co particle size (nm)		Reduction degree[c] (%)			
	XRD[a]	TEM[b]	TPR[d]	O_2 titration[e]	H_2 uptake[f] (μmol g^{-1})	Dispersion[g] (%)
Co/SiO_2	7.9	10.1	39.9	34.1	28.2	9.6
Co/SiO_2 (EG)	N.A.	3.4	20.8	19.2	17.5	28.1
$Co–Ru/SiO_2$	9.5	10.7	74.1	78.1	45.9	8.9
$Co–Ru/SiO_2$ (EG)	N.A.	3.8	63.1	61.2	99.9	25.3

[a] From XRD patterns of passivated catalysts. [b] From TEM images of passivated catalysts. [c] Assuming the noble metal was completely reduced at 673 K. [d] Determined by TPR profiles from 323 K to 673 K. CuO was used as reference sample. [e] Determined by O_2 titration at 673 K. [f] Determined by H_2 chemsorption at 373 K. [g] Dispersion was calculated by $D = 96/d(\mathrm{Co})$ (%). d(Co) was Co particle size.

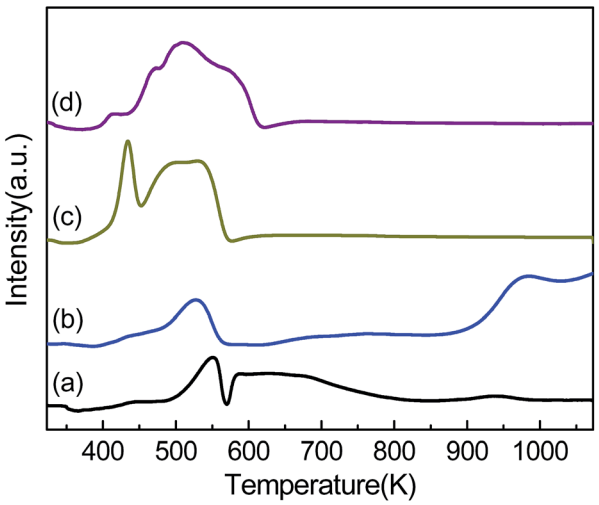

Fig. 3 TPR profiles of the prepared catalysts: (a) Co/SiO_2, (b) Co/SiO_2 (EG), (c) $Co–Ru/SiO_2$, and (d) $Co–Ru/SiO_2$ (EG).

the supported cobalt oxide difficult to be reduced (19.2% reduction degree), which was due to the formation of small Co particles on the surface of EG-modified silica support. For Ru added $Co–Ru/SiO_2$ and $Co–Ru/SiO_2$ (EG) catalysts, the reduction degree was much higher than that of Co/SiO_2 and Co/SiO_2 (EG) catalysts, indicating that addition Ru could effectively enhance the reducibility of cobalt oxide, contributing to forming much more cobalt active sites. The H_2 chemsorption results, as shown in Table 1, proved that the $Co–Ru/SiO_2$ (EG) catalyst realized the maximum of H_2 uptake as 99.9 μmol g^{-1}, indicating that this catalyst formed the most active sites in this study, meanwhile, the H_2 uptake of Co/SiO_2 (EG) catalyst is the lowest in Table 1.

The XPS study was carried out to determine the chemical composition and valence state of the elements on the surface of cobalt oxide. As shown in Fig. 4, from Co 2p core level spectrum of the catalyst Co/SiO_2, two peaks located near 780.30 and 795.73 eV are observed. These two peaks come from the spin–orbit splitting and can be attributed to Co $2p_{3/2}$ and Co $2p_{1/2}$, respectively.[22] At the same time, two shake-up satellite peaks, which arise from the presence of unpaired electrons in valence orbital, appear in the spectra of Co 2p at about 5–7 eV higher energy side from the Co $2p_{3/2}$ and Co $2p_{1/2}$ peaks, indicating the presence of Co^{2+} on the surface of catalyst.[23] The similar results were also observed in Co 2p spectra of the other three catalysts.

It is shown that EG pretreatment caused Co $2p_{3/2}$ and Co $2p_{1/2}$ peaks to appear at relatively higher binging energy. This result indicated a stronger interaction between SiO_2 support and cobalt oxide species and an electron transfer from cobalt oxide to support for EG-modified catalysts, contributing to a smaller particle size and low electron density of cobalt oxide.[14,24] Addition of Ru shifted the Co 2p peaks of Ru added catalysts to lower binding energy, indicating that the addition of Ru increased the electron density of supported Co ions.

In situ CO-DRIFT spectra of the reduced catalysts are compared in Fig. 5. For Co/SiO_2 catalyst, an intense peak at 2034 cm^{-1} and weak peaks at 1934, 2117 cm^{-1} were observed. The 2034 cm^{-1} peak was assigned to CO adsorbed on cobalt metal in a linear geometry. The 1934 cm^{-1} peak was due to the bridge-type CO on Co sites. The peak at 2117 cm^{-1} was assigned to the CO adsorbed on Co^{n+} ($n = 2$ and 3) species.[18] It was shown that the linear-adsorbed CO peak of Co/SiO_2 (EG) shifted to higher position to 2040 cm^{-1}, indicating the small cobalt particles for this catalyst.[25] On the other hand, the low intensity of all CO adsorption bands and the high intensity of CO–Co^{n+} species on Co/SiO_2 (EG) indicated that there were more

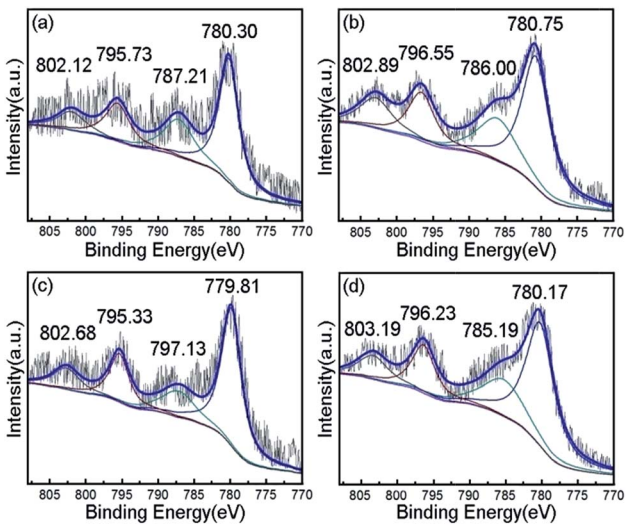

Fig. 4 XPS spectra of Co 2p core level recorded from prepared catalysts: (a) Co/SiO_2, (b) Co/SiO_2 (EG), (c) $Co–Ru/SiO_2$, and (d) $Co–Ru/SiO_2$ (EG).

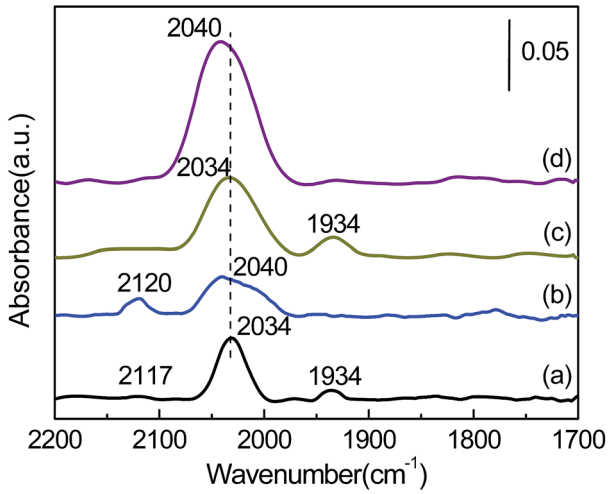

Fig. 5 CO-DRIFT spectra of various catalysts: (a) Co/SiO_2, (b) Co/SiO_2 (EG), (c) $Co–Ru/SiO_2$, and (d) $Co–Ru/SiO_2$ (EG).

unreduced Co ions on the surface of Co/SiO_2 (EG) catalyst due to the low reduction degree as compared in Table 1.

For the Ru added catalysts, the $Co–Ru/SiO_2$ catalyst exhibited stronger linear- and bridged-adsorbed CO peaks than Co/SiO_2 due to the higher reduction degree, and very similar adsorbed CO location to Co/SiO_2 due to similar cobalt particle size of $Co–Ru/SiO_2$. On the other hand, $Co–Ru/SiO_2$ (EG) catalyst exhibited the strongest adsorption band and obvious blue shift for linear-type CO peak. These linear-type adsorbed CO molecules at high wavenumber (2040 cm^{-1}) preferred to non-dissociative CO insertion events, which is advantageous to CO insertion reaction and would contribute to hydroformylation reaction.[26] Moreover, the intensity of linear-bonded CO peak for $Co–Ru/SiO_2$ (EG) was much stronger than that for $Co–Ru/SiO_2$, because the smaller Co particles and high reduction degree of this catalyst resulted in much more active sites, contributing to higher activity of 1-hexene hydroformylation.

The prepared catalysts were tested in slurry phase hydroformylation of 1-hexene under 403 K and 5 MPa, and the reaction results were compared in Table 2.

As comparison, SiO_2 supported 1 wt% Ru catalyst was also tested in 1-hexene hydroformylation. As shown in Table 2, both Ru/SiO_2 catalysts exhibited very low catalytic activity of hydroformylation, resulting in less than 1% heptanal yield, indicating that the Ru was not active in hydroformylation of 1-hexene. Therefore, in this study, it is considered that the added Ru only improved the reduction degree of supported cobalt and did not contribute the catalytic activity of hydroformylation. For the Co/SiO_2 catalyst, due to large particle size and much less amount of active sites, the conversion of 1-hexene and yield of heptanal were very low in 1-hexene hydroformylation. Meanwhile, even though the Co/SiO_2 (EG) catalyst realized very small cobalt particle size, due to the lowest reduction degree this catalyst formed the minimum of active sites as compared in Table 1, resulting in the lowest heptanal yield in this study.

On the other hand, as is shown in Table 2, the $Co–Ru/SiO_2$ (EG) catalyst realized 3 times higher 1-hexene conversion as 93.01% and 18 times higher heptanal yield as 74.09% than conventional Co/SiO_2 catalyst. It is reported that the atoms at the corners and edges of metal particles are advantageous to CO adsorption in linear geometry, which benefit the CO insertion during the hydroformylation reaction.[26,27] Because the EG modification of silica support significantly improved the dispersion of supported cobalt and formed smaller cobalt particle, smaller particle size of $Co–Ru/SiO_2$ (EG) catalyst, where the number of atoms at the corners and edges of metal particles was more, was beneficial for improving the catalytic activity of 1-hexene hydroformylation. On the other hand, smaller particle size of supported cobalt was advantageous for linear type CO adsorption, which was more active in CO insertion reaction. Meanwhile, the added Ru significantly improved the reducibility of highly dispersed cobalt, contributing to the highest 1-hexene conversion. Based on mentioned above, the $Co–Ru/SiO_2$ (EG) catalyst realized the highest 1-hexene conversion and yield of heptanal. For the $Co–Ru/SiO_2$ catalyst, the added Ru promoted the reduction degree, contributing to improve the activity of 1-hexene hydroformylation, resulting in relatively higher 1-hexene conversion. However, the largest cobalt particle size of $Co–Ru/SiO_2$ catalyst was disadvantageous to CO insertion reaction, leading to much lower yield of heptanal than that of $Co–Ru/SiO_2$ (EG) catalyst. The stability of $Co–Ru/SiO_2$ (EG) catalyst in terms of heptanal yield is shown in Fig. S1.† After 5 reaction entry, the activity of $Co–Ru/SiO_2$ (EG) catalyst is still high and do not exhibit obvious decrease, which should be due

Table 2 Reaction performances of 1-hexene hydroformylation over various catalysts[a]

		Selectivity/%						
Catalyst	Conv.[b]/%	*n*-Hexane	Iso-hexene	*n*-Heptanal	Iso-heptanal	Total[c]	Yield[d]/%	*n*/iso[e]
Co/SiO_2	32.69	0.00	85.37	8.94	5.69	14.63	4.78	1.75
Co/SiO_2 (EG)	28.34	0.00	89.56	6.06	4.38	10.44	2.96	1.39
$Co–Ru/SiO_2$	50.27	8.37	32.19	41.12	18.32	59.44	29.88	2.37
$Co–Ru/SiO_2$ (EG)	93.01	4.16	16.18	55.84	23.82	79.66	74.09	2.34
Ru/SiO_2	6.80	51.22	38.91	7.01	2.86	9.87	0.67	2.45
Ru/SiO_2 (EG)	7.37	46.75	42.57	7.71	2.97	10.68	0.79	2.57

[a] Reaction conditions: $CO : H_2 = 1 : 1$, 403 K, 5 MPa, 1 h, 20 mL of toluene, 13.5 mmol of 1-hexene, catalyst loading = 0.1 g. [b] Conversion of 1-hexene. [c] Total selectivity of *n*-heptanal and iso-heptanal. [d] Yield of *n*-heptanal and iso-heptanal. [e] *n*/iso: *n*-heptanal/iso-heptanal.

to the low cobalt leaching. The strong interaction between supported cobalt particles and SiO_2 prevents the formation of soluble cobalt species such as cobalt carbonyls which lead to the elution of cobalt.[16,28] On the other hand, as shown in Table S1,† the BET surface area of the passivated and the spent catalysts exhibited negligible changes, which is benefit for the stability of catalyst.

Conclusions

A highly dispersed cobalt catalyst was successfully obtained by pretreating SiO_2 with EG and adding small amount of noble metal Ru. The Co–Ru/SiO_2 (EG) catalyst realized excellent reaction performance in 1-hexene hydroformylation, such as 93.01% 1-hexene conversion and 74.09% heptanal yield. The promotional effects of EG pretreatment and Ru addition on the catalytic performances of the obtained catalysts were investigated by several characterization methods. The results indicated that pretreatment SiO_2 with EG significantly enhanced the interaction between cobalt precursor and support, resulting in high dispersion but low reduction degree. Addition of trace amount of Ru could remarkably improve the reduction degree. High dispersion and reduction degree of Co–Ru/SiO_2 (EG) contributed to forming the large number of active sites and more linear-adsorbed CO molecules with strong C–O bond, which were benefit for the catalytic activity in 1-hexene hydroformylation. Therefore, under the promotional effects of EG and Ru, Co–Ru/SiO_2 (EG) catalyst realized the best catalytic activity in 1-hexene conversion and heptanal yield in this study.

Acknowledgements

Financial support from the National Natural Science Foundation of China (no. 91334206 and 51174259), Ministry of Education of People's Republic of China (NCET-13-0653), National "863" program of China (no. 2012AA051001 and 2013AA031702) is greatly appreciated.

Notes and references

1 A. Neves, M. Calvete, T. Pinho e Melo and M. Pereira, *Eur. J. Org. Chem.*, 2012, **32**, 6309–6320.
2 R. Franke, D. Selent and A. Borner, *Chem. Rev.*, 2012, **112**, 5675–5732.
3 Q. Cai and J. L. Li, *Catal. Commun.*, 2008, **9**, 2003–2006.
4 S. R. Wang, Q. Q. Yin, J. F. Guo, B. Ru and L. J. Zhu, *Fuel*, 2013, **108**, 597–603.
5 H. Arakawa, N. Takahashi, T. Hanaoka, K. Takeuchi, T. Matsuzaki and Y. Sugi, *Chem. Lett.*, 1988, **17**, 1917–1918.
6 X. G. Song, Y. J. Ding, W. M. Chen, W. D. Dong, Y. P. Pei, J. Zang, L. Yan and Y. Lu, *Appl. Catal., A*, 2013, **452**, 155–162.
7 E. Iglesia, S. L. Soled and R. A. Fiato, *J. Catal.*, 1992, **137**, 212–224.
8 B. G. Johnson, C. H. Bartholomew and D. W. Goodman, *J. Catal.*, 1991, **128**, 231–247.
9 M. K. Gnanamani, G. Jacobs, W. D. Shafer and B. H. Davis, *Catal. Today*, 2013, **215**, 13–17.
10 (*a*) A. H. Kababji, B. Joseph and J. T. Wolan, *Catal. Lett.*, 2009, **130**, 72–78; (*b*) N. Kumar, E. A. Payzant, K. Jothimurugesan and J. J. Spivey, *Phys. Chem. Chem. Phys.*, 2011, **13**, 14735–14741.
11 (*a*) E. Escalera, M. A. Ballem, J. M. Cordoba, M. Antti and M. Oden, *Powder Technol.*, 2012, **221**, 359–364; (*b*) G. Mitran, T. Cacciaguerra, S. Loridant, D. Tichit and I. Marcu, *Appl. Catal., A*, 2012, **417–418**, 153–162; (*c*) F. Ioana, D. Saida, M. Rima, H. Oana, L. Liliana, L. Doina, B. Ion and G. Francois, *Environ. Eng. Manage. J.*, 2012, **11**, 1931–1943.
12 Y. Zhang, K. Hanayama and N. Tsubaki, *Catal. Commun.*, 2006, **7**, 251–254.
13 Y. Zhang, Y. Liu, G. H. Yang, Y. Endo and N. Tsubaki, *Catal. Today*, 2009, **142**, 85–89.
14 J. F. Chen, Y. R. Zhang, L. Tan and Y. Zhang, *Ind. Eng. Chem. Res.*, 2011, **50**, 4212–4215.
15 X. Y. Lv, J. F. Chen, Y. S. Tan and Y. Zhang, *Catal. Commun.*, 2012, **20**, 6–11.
16 Y. Zhang, K. Nagasaka, X. Q. Qiu and N. Tsubaki, *Catal. Today*, 2005, **104**, 48–54.
17 J. J. Rodrigues, G. Pecchi, F. A. N. Fernandes and M. G. F. Rodrigues, *J. Nat. Gas Chem.*, 2012, **21**, 722–728.
18 N. Tsubaki, S. L. Sun and K. Fujimoto, *J. Catal.*, 2001, **199**, 236–246.
19 (*a*) G. Jacobs, T. K. Das, Y. Q. Zhang, J. L. Li, G. Racoillet and B. H. Davis, *Appl. Catal., A*, 2002, **233**, 263–281; (*b*) E. Finocchio, I. Rossetti and G. Ramis, *Int. J. Hydrogen Energy*, 2013, **38**, 3213–3225.
20 D. Y. Xu, W. Z. Li, H. M. Duan, Q. J. Ge and H. Y. Xu, *Catal. Lett.*, 2005, **102**, 229–235.
21 N. Eacalona, C. Medina, R. Garcia and P. Reyes, *Catal. Today*, 2009, **143**, 76–79.
22 (*a*) Z. G. Liu, S. H. Chai, A. Binder, Y. Y. Li, L. T. Ji and S. Dai, *Appl. Catal., A*, 2013, **451**, 282–288; (*b*) E. Meza, J. Ortiz, D. Ruiz-Leon, J. F. Marco and J. L. Gautier, *Mater. Lett.*, 2012, **70**, 189–192.
23 T. Mochizuki, T. Hara, N. Koizumi and M. Yamada, *Appl. Catal., A*, 2007, **317**, 97–104.
24 N. Koizumi, T. Mochizuki and M. Yamada, *Nanotechnology*, 2009, **7**, 633–640.
25 S. L. Sun, N. Tsubaki and K. Fujimoto, *Chem. Lett.*, 2000, **29**, 176–177.
26 Y. Zhang, M. Shinoda, Y. Shiki and N. Tsubaki, *Fuel*, 2006, **85**, 1194–1200.
27 N. Takahashi, T. Tobise, I. Mogi, M. Sasaki, A. Mijin, T. Fujimoto and M. Ichikawa, *Bull. Chem. Soc. Jpn.*, 1992, **65**, 2565–2567.
28 T. A. Kainulainen, M. K. Niemela and A. O. I. Krause, *J. Mol. Catal. A: Chem.*, 1997, **122**, 39–49.

